AD-A105 318   BATTELLE COLUMBUS LABS OH   F/G 20/1

ACOUSTIC ANALYSIS TECHNIQUES FOR NAVY GYROSCOPE BALL BEARINGS.(U)

APR 74   T A DOW, W A GLAESER, J W KISSEL   N62269-71-C-0601

UNCLASSIFIED   NL

1 OF 1

AD A105318

END

DATE FILMED

11-81

DTIC

LEVEL II

AERONAUTICAL ANALYTICAL REWORK PROGRAM SUMMARY REPORT

ACOUSTIC ANALYSIS TECHNIQUES FOR NAVY GYROSCOPE BALL BEARINGS

APRIL 26, 1974

CONTRACT N62269-71-C-0601

by

T. A. Dow, W. A. Glaeser, J. W. Kissel,
G. K. Nessler, and D. K. Snediker

to

ANALYTICAL REWORK/SERVICE LIFE PROJECT OFFICE

NAVAL AIR DEVELOPMENT CENTER, WARMINSTER, PA. 18974

AERONAUTICAL ANALYTICAL REWORK PROGRAM

(1) SUMMARY REPORT

(6) ACOUSTIC ANALYSIS TECHNIQUES FOR NAVY
GYROSCOPE BALL BEARINGS.

to

ANALYTICAL REWORK/SERVICE LIFE PROJECT OFFICE
NAVAL AIR DEVELOPMENT CENTER
WARMINSTER, PA. 18974

(11) 26 Apr~~il 26~~, 1974 (12) 24

(15)

Contract N62269-71-C-0601

by

(10) T. A. Dow, W. A. Glaeser, J. W. Kissel
G. K. Nessler ~~and~~ D. K. Snediker

BATTELLE
Columbus Laboratories
505 King Avenue
Columbus, Ohio 43201

405080 B

TABLE OF CONTENTS

AERONAUTICAL ANALYTICAL REWORK PROGRAM

SUMMARY REPORT

ACOUSTIC ANALYSIS TECHNIQUES FOR NAVY
GYROSCOPE BALL BEARINGS

to

ANALYTICAL REWORK/SERVICE LIFE PROJECT OFFICE
NAVAL AIR DEVELOPMENT CENTER
WARMINSTER, PA. 18974

from

BATTELLE
Columbus Laboratories

April 26, 1974

SUMMARY

In an effort to develop a method for the acoustic characterization of gyro bearings (both as components and at various stages of the gyro buildup), a study of one promising method was carried out. Sensitive (and discriminating) acoustic analysis (AA) of miniature bearings has usually involved the rigorous application of narrow-band frequency analysis interpreted by means of a sophisticated and involved mathematical model. Such a technique, however rigorous it may be, is too slow and complex for use in a production facility by relatively untrained personnel.

Of the several real-time, broad-band frequency-analysis methods available, the high-frequency resonance technique was determined by testing actual NARF reject bearings and new bearings, to have the greatest potential for meeting USN requirements. This technique involves the measurement of high-frequency structural resonances in the fixture. These resonance peaks, excited by damage impacts in the test bearing, occur at frequencies sufficiently high (30-50 KHz) that background noise is very low and a good signal-to-noise ratio is obtained.

This method has potential for development into a simple, inexpensive instrument for use in screening bearings and for inspecting gyro assemblies.

INTRODUCTION

In a recent survey conducted for the Analytical Rework Program ("An Analysis of Maintenance Procedures and Problems Involving Miniature Precision Bearings in Naval Avionics Equipment and Aeronautical Instruments"), it was found that an efficient and reliable method was needed to certify miniature precision bearings for instrument and gyroscope applications. Test devices in use at present have not proven satisfactory because either they are too complex and time consuming or they do not detect all critical bearing defects. In addition, there is no test device which can check out a bearing during buildup of a gyro. Considerable time must be invested in completing a gyro buildup before the gyro can be tested to see if the bearings have been installed correctly and not damaged or contaminated during installation. The survey recommended that "inspection with acoustic-signature analysis (ASA) is considered to be a more complete and objective technique for determining overall bearing suitability".

To carry out this recommendation, a program has been initiated to develop an ASA bearing qualification system adapted to the specific requirements for miniature precision bearing maintenance in the Analytical Rework Program.

The determination of the condition of a machine by means of its acoustic emissions is a diagnostic technique as old as machines themselves. Just after World War II, an effort was made to replace the trained mechanic's ear with an instrumented method that could reliably determine the condition of a mechanism quantitatively and, furthermore, pinpoint the problem area. In spite of intensive research and development over the past 25 years, the analysis of mechanical acoustic emissions as represented by ASA has not found wide application as a general mechanical diagnostic technique. In certain areas, however, the technique

has been applied successfully to relatively simple, precision, mechanisms. One such area is the determination of the condition of gyroscope bearings under laboratory conditions[1]*.

Three general approaches have been used in the acoustic analysis of precision bearing systems--

- Narrow band frequency analysis (NBFA) wherein a high-resolution acoustic spectrum of fundamental defect frequencies and harmonics is analyzed using a comprehensive mathematical model of the bearing. This method does not lend itself easily to real-time analysis and requires relatively sophisticated software.[1,2]
- Broad-band frequency analysis (BBFA) (typified by the approach used in Reference 4), is a technique that has been used successfully for real-time analyses. The technique is similar to NBFA in that bearing condition is determined by analysis of an acoustic spectrum consisting of defect frequencies and their harmonics. A spectrum analyzer having less resolution than that required for rigorous NBFA is employed to give real-time analysis capability. This technique does not allow the same level of defect assignment as does NBFA and requires relatively sophisticated hardware.
- Other methods have been employed for acoustic analysis. Two such methods are structural-resonance analysis (SRA)[3] and high-frequency analysis (HFA). The former method uses the hardware surrounding the bearing as a resonant detector. Defect impacts in the bearing excite structural resonances that can be measured using relatively simple equipment. The latter method correlates ultrasonic emissions from stressed metals with incipient failure (generally metals failing or failed by fatigue).

Applying the ASA to gyro bearings on a production basis is presently without precedent. ASA has been applied successfully to gyro bearings and

*References are on Page 20.

float-level assemblies in the laboratory (see for example Reference 1); however, no present gyro rework processes make use of instrumented acoustic methods. We recognize certain critical requirements in the adaptation of present methods to a gyro production application. These requirements are the basic criteria against which the state of the art in acoustic analysis has been evaluated for this program and against which the new techniques developed must be compared continually. These critical requirements are summarized in Table 1.

TABLE 1. CRITICAL REQUIREMENTS FOR AN ASA METHOD TO BE APPLIED TO NAVAL GYRO REWORK PROCESSES

- The method must be simple to operate. Regular NARF personnel must be capable of carrying out the analysis and interpretation.
- The results must be unequivocal, with a minimum of judgement and engineer/supervisor involvement.
- The method should be fail-safe such that bad bearings do not pass.
- The first cost and operating cost of the equipment should be relatively low, ideally not exceeding present NARF diagnostic systems.
- The method should be capable of high production rates with a minimum of exposure of the bearings to damage and contamination.

A survey of the state of the art in acoustic bearing analysis relative to these requirements would seem to eliminate *a priori* the candidacy of most narrow-band techniques and ultrasonic methods. The techniques involved are relatively complex and these techniques seem *not* to deal with relevant gyro bearing defect conditions. Thus, this study focused on the broad-band, real-time methods and the resonance methods that offered potential in meeting most, if not all, of the critical requirements.

The general approach was to generate a mathematical model for the expected acoustic spectrum of a ball bearing and use this model to determine the frequencies of common defects in a Navy gyro (R4) bearing. These results were then used to design a test fixture and to define an experimental approach. The theoretical spectrum was also used to aid in the understanding of the experimental spectra. Several candidate test methods were then implemented and evaluated with regard to their ability to discriminate bad from good bearings, and for potential for development into hardware and methodology meeting the critical requirements summarized in Table 1.

ANALYSIS

A defect-frequency analysis was carried out in which the major forcing frequencies of a ball-bearing system are predicted. The method employed is based on prior work (Reference 1 and 2) and involves the determination of the frequencies of specific geometrical defects; i.e., race scratch, ball scratch, out-of-round ball, etc. The characteristic frequency associated with a single defect, as well as those for multiples of that defect are calculated for a given bearing geometry.

The frequencies predicted have been developed from a geometric study of the bearing. For example, consider the case of a single scratch on the outer race of an inner-race rotating bearing. If the bearing contained only a single ball, it would strike that scratch once per revolution of the cage, because the ball is constrained to move with the cage. However, a ball bearing actually contains many balls so that the frequency associated with a single outer race scratch will be the cage frequency times the number of balls, (N). The cage frequency is dependent upon the geometry of the bearing, i.e., the ball and pitch diameters, denoted by d and D, respectively, and the contact angle of the balls and race, denoted by β. The cage frequency (f_c) will then be:

$$f_c = \frac{\omega_i}{2}\left[1 - \frac{d}{D}\cos\beta\right] \qquad (1)$$

where ω_i is the inner-race rotation frequency (cps). Therefore, the defect frequency (f_D) of a single scratch on the outer race will be

$$f_D = \frac{N\omega_i}{2}\left[1 - \frac{d}{D}\cos\beta\right] \quad . \qquad (2)$$

If more than one scratch were present on the outer race of the bearing, the defect frequency would be some multiple of that shown in Equation 2. Other geometric defects such as a scratch on the ball or an out-of-round ball can be modeled by a similar procedure.

Table 2 shows the defect frequency relationships associated with specific bearing defects. The linear frequencies are based on a linear deformation model of ball-race contacts. The nonlinear effects are associated with nonlinear deformation of the bearing structure. An example calculation for a bearing used in these experiments is shown in Table 3. The particular defect is described on the left hand side of the print out and the frequency of single and multiple defects are shown opposite it. The frequencies are given as multiples of the inner race rotation frequency.

The vibration due to a single defect predicted from the analysis may or may not be visible on a frequency spectrum of a bearing even if that defect is intentionally introduced into the bearing. The reason is that the defect vibration acts as a forcing function and the output of the accelerometer (from which the frequency spectrum is obtained) is related to its mounting on the bearing housing. If a bearing could be isolated such that no housing was necessary, the forcing frequencies--bearing defect frequencies--would be visible. However, the housing characteristics change the applied signal and can be thought of as transfer functions which modify the applied vibration. As a result, the forcing frequencies may exhibit themselves as beat frequencies superimposed on the higher frequency portion of the spectrum or they may modify the amplitude of the natural frequency vibration of the housing.

TABLE 2. BEARING DEFECTS BY LINEAR AND NONLINEAR ANALYSIS

Surface Defect		Vibrational Orders	
Ball Part	Imperfection	Linear Theory	Nonlinear Theory
	Eccentricity[a]	1	--
Inner race	Waviness[b]	$mNf_i \pm 1$	$mf_i \pm f_c$
	Rough spot	mNf_i	--
Outer race	Waviness; rough spot	mNf_c	$(m \pm 1) f_c$
	Diameter variation	f_c	--
Ball	Waviness	$2mf_b \pm f_c$	--
	Rough spot	$2mf_b$	--

(a) 1 wave per revolution.

(b) Multiple waves per revolution.

Where f_b = Ball rotation frequency = $\frac{D}{2d}\left[1 - \left(\frac{d}{D}\right)^2 \cos^2 \beta\right]$

f_i = Cage rotation with respect to rotating inner race = $\frac{1}{2}\left[1 + \left(\frac{d}{D}\right) \cos \beta\right]$

m = Multiple defect index (n = 1, 2, 3, ...).

```
RPM OF INNER RACE = 2750.00
THRUST LOAD(T) =      4.00  LBS.
TOTAL CURVATURE(B) =      0.04  IN.
DIAMETER OF BALL (DB) =      0.09  IN.
PITCH DIAMETER(E) =      0.41  IN.
INITIAL CONTACT ANGLE(BETAI) =     12.80  DEGREES
NUMBER OF BALLS(N) =     8

K =  0.1123E+06      DIMENSIONLESS LOAD(TP) =  0.5066E-03
0.1088E+00  0.7496E+00  0.7224E+00  0.5783E+00
0.3596E-01  0.3086E+00  0.5783E+00  0.4618E+00
0.1137E-01  0.1321E+00  0.4618E+00  0.3757E+00
0.3383E-02  0.5985E-01  0.3757E+00  0.3192E+00
0.8865E-03  0.3047E-01  0.3192E+00  0.2901E+00
0.1647E-03  0.1957E-01  0.2901E+00  0.2816E+00
0.1152E-04  0.1686E-01  0.2816E+00  0.2810E+00
OPERATING CONTACT ANGLE =    16.10  DEGREES

     THE FOLLOWING FREQ(HERTZ) WILL BE THE MAJOR
FREQUENCIES OF THE ACOUSTIC SIGNATURE OF THE BEARING

INNER RACE FREQ(FI) =     45.83
CAGE FREQ(FC) =     17.88
CAGE RELATIVE TO INNER FREQ(FCI) =     27.95
BALL ROTATION FREQ(FB) =     95.39

     POSSIBLE VIBRATION ORDERS AND THEIR SOURCES

BEARING IMPERFECTION                               VIBRATION ORDER
********************                               ***************

INNER RING ECCENTRICITY                                  1.00

INNER RACE WAVINESS          LINEAR                      5.88
                                                         3.88
                             NONLINEAR
                                                   0.22        1.00
                                                   0.83        1.61
                                                   1.44        2.22
                                                   2.05        2.83
                                                   2.66        3.44
                                                   3.27        4.05
                                                   3.88        4.66
                                                   4.49        5.27
                                                   5.10        5.88
                                                   5.71        6.49
                                                   6.32        7.10
                                                   6.93        7.71
                                                   7.54        8.32
                                                   8.15        8.93
                                                   8.76        9.54
                                                   9.37       10.15

OUTER RACE WAVINESS          LINEAR                      3.12
                             NONLINEAR
                                                   0.00        0.78
                                                   0.39        1.17
                                                   0.78        1.56
                                                   1.17        1.95
                                                   1.56        2.34
                                                   1.95        2.73
                                                   2.34        3.12
                                                   2.73        3.51
                                                   3.12        3.90
                                                   3.51        4.29
                                                   3.90        4.68
                                                   4.29        5.07
                                                   4.68        5.46
                                                   5.07        5.85
                                                   5.46        6.24
                                                   5.85        6.63
                                                   6.24        7.02
                                                   6.63        7.41
                                                   7.02        7.80
                                                   7.41        8.19
                                                   7.80        8.58
                                                   8.19        8.97
                                                   8.58        9.36
                                                   8.97        9.75
                                                   9.36       10.14

 BALL DIAMETER VARIATION                                  0.39

 BALL WAVINESS                                     3.77        4.55
 BALL WAVINESS                                     7.93        8.71

 BALL DEFECT                                              2.08
                                                          4.16
                                                          8.32
                                                         12.49
```

TABLE 3. COMPUTER PRINTOUT OF TEST BEARING ANALYSIS

EXPERIMENTAL METHOD

Bearing Test Apparatus

The bearing test fixture, Figure 1a, consisted of a rigid-plate frame in which the test bearing was mounted with its spin axis vertical. The upper plate supported the outer race of the bearing, while a 10-lb dynamically balanced shaft was hung from the inner race. Thus, the shaft provided a constant, known thrust load. The bottom of the shaft was carried in a self-aligning bronze cylindrical bearing which supported no axial load. The shaft was driven through an O-ring belt from a remotely-mounted motor; therefore, the test bearing is the only ball bearing on the fixture.

A piezoelectric accelerometer (manufactured by Columbia) was installed on the test-bearing mounting block as illustrated in Figure 1b. The orientation was chosen for maximum sensitivity in a radial direction with respect to the test bearing.

The initial attempt at obtaining a bearing-signature to determine bearing defects was with a 1/10 octave band-swept General Radio filter. This method proved inadequate for distinguishing discrete frequency peaks--due to the wide band-width of the filters. It was found that throughout the first ten harmonic orders of the rotational speed of the bearing (46 to 460 Hz) most of the resonance peaks merged to an extent which permitted very little extraction of information pertinent to bearing condition or damage to its rolling elements.

In order to better resolve the bearing defect spectrum while maintaining a reasonably short analysis time, a real time spectrum analyzer was employed. This instrument, a Federal Scientific UA 500, provided 0.01 percent resolution from nominally DC to 100,000 Hz. The ancillary instrumentation consisted of an Umholtz-Dickie charge amplifier, with a 100,000 Hz-frequency response, and an x-y plotter. These instruments provided 500-line delineation of acceleration amplitudes for a series of frequency rangles extending from 1 to 100 K Hz. The Real Time Analyzer also provided for manual selection of the number of spectra to be averaged

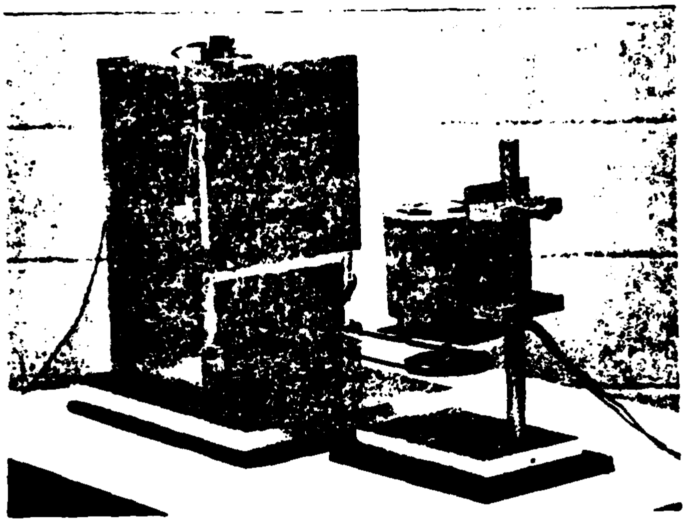

(a) Fixture with Motor Drive

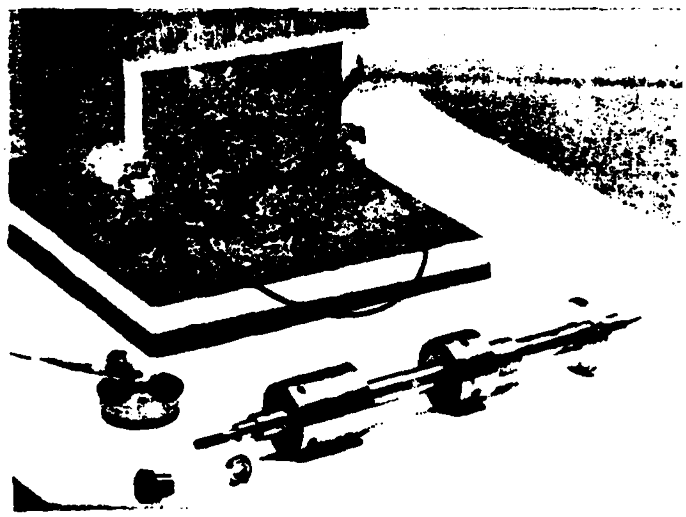

(b) Fixture--Showing Balanced Shaft, Test Bearing and Accelerometer Mount

FIGURE 1. BEARING TEST FIXTURE

for a given spectral plot. To standardize the experimental technique employed for the bearing comparisons, 32 spectra were averaged for plots encompassing 0 to 500 Hz, and 128 spectra were averaged for each of the plots, 0 to 5000 Hz, and 0 to 50,000 Hz. (The lower number, 32, was chosen because of the long time required for data accumulation in the low-frequency range.) In order to provide the multiple experimental spectral plots illustrated in Figures 2a and 2b, each bearing was operated in the fixture for approximately 20 minutes. An individual spectrum took about 6 minutes for the low frequency range and about 5 minutes for the middle and high ranges.

Experimental Bearings

All bearings were SR4 size but several different manufacturers were represented and the design with respect to shielding was not identical throughout.

Five of the "failed" bearings, provided by the Navy, were compared with two new bearings and also with two bearings which were intentionally damaged. The two new bearings were Barden type-VR4SSW4V (passed by Smootherator Test), three of the "failed" Navy bearings (7B, 13A, and 23C) were also Barden--presumably the same type (double shielded). The remaining two "failed" Navy bearings (13 C and 14CC) were manufactured by New Hampshire Ball Bearing Company (NHBB). The intentionally damaged bearings were: an NHBB SR4 not manufactured to Navy specifications and a New Departure bearing from the standard inventory. The NHBB bearing was damaged by applying a light-hammer blow to the outer race, thereby causing brinelling of races and possibly flattening on one or more balls. The New Departure bearing was disassembled and three very close transverse scratches were scribed across the outer race ball track area. The effect of these scratches on the resonance spectra varied with the direction of axial load application. Reasonable care was taken to maintain the cleanliness of the bearings, however, no cleaning and relubrication was carried out, except for the ND bearing that had been disassembled for scribing.

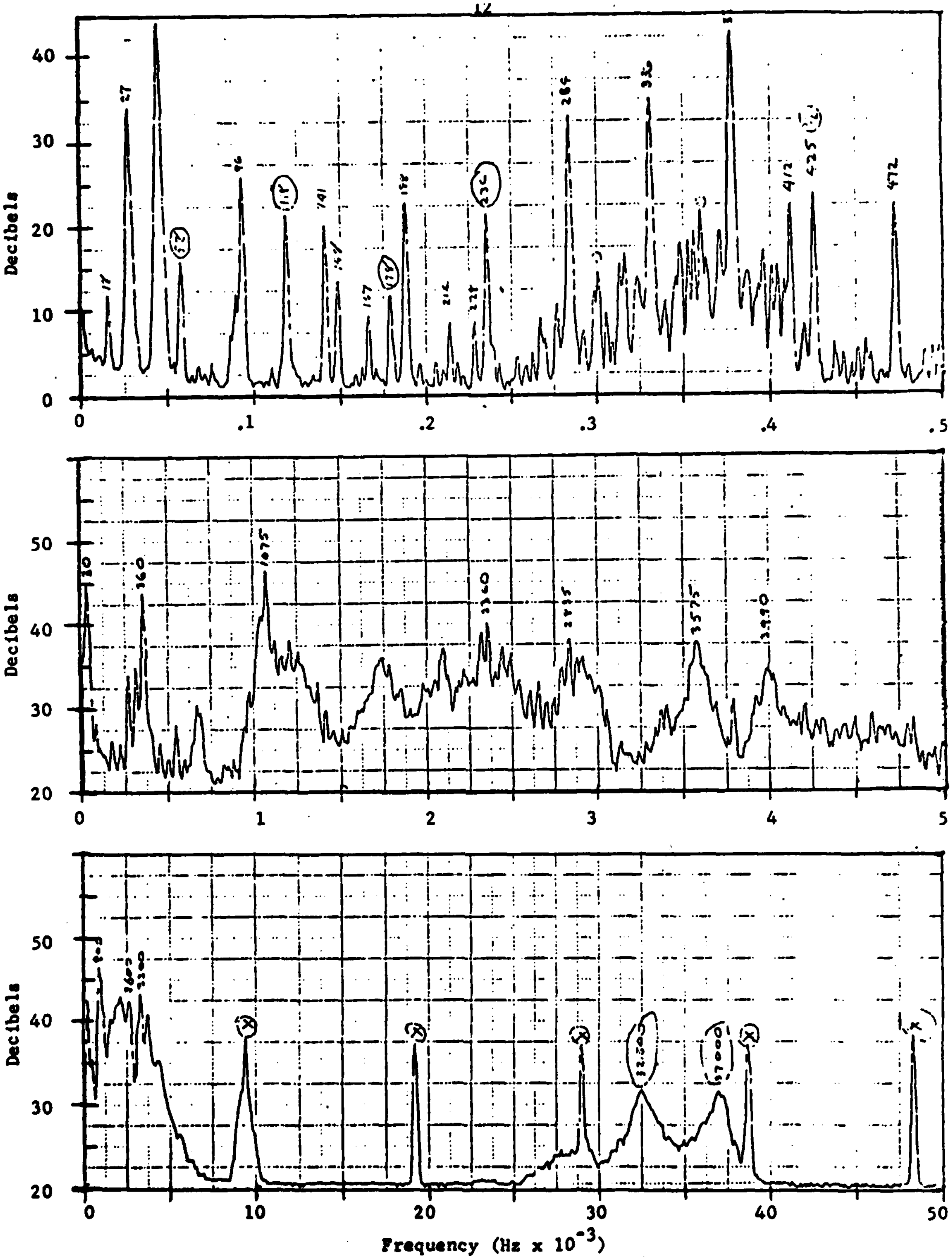

FIGURE 2a. ACCELERATION SPECTRA (1 TO 50,000 HZ) FOR BEARING C - NEW BEARING

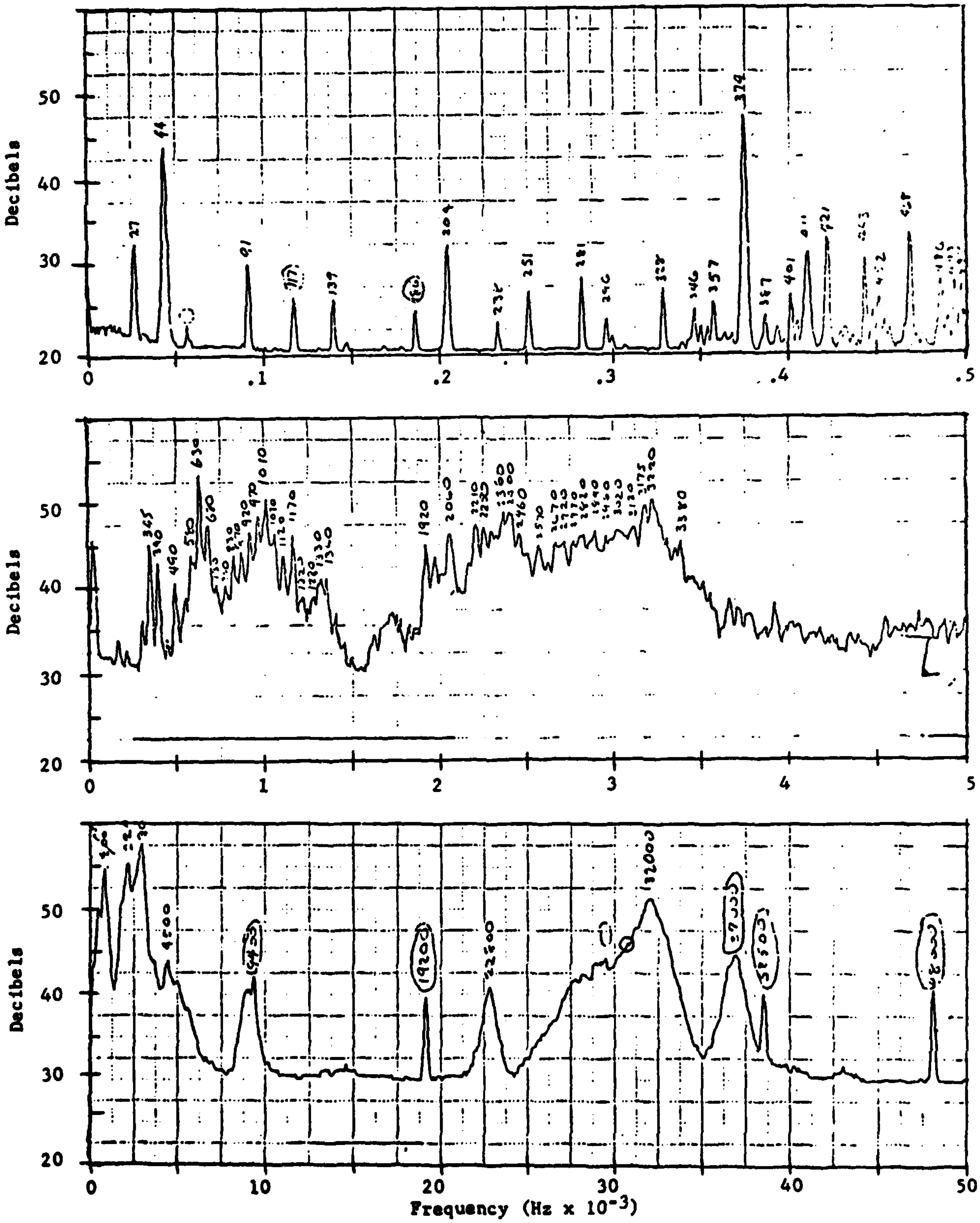

FIGURE 2b. ACCELERATION SPECTRA (1 TO 50,000 HZ) FOR BEARING J_1 - WITH SCRATCH IN OUTER RACE

EXPERIMENTAL RESULTS

The acceleration-spectra plots (Figures 2a and 2b) contain peaks from several sources: (1) bearing rolling-element impacts, (2) structural resonances of the bearing support fixture, (3) electronically produced artifacts originating in the analytical components, and (4) mechanically-induced resonance of the accelerometer pickup.

These spectra were analyzed in several ways. The first, and most obvious, was to compare the fundamental and lower harmonics for those frequencies determined by the analysis to result from race and ball defects. A plot of resonance-peak amplitude and density for four of the experimental bearings is shown in Figure 3. This presentation demonstrates a very considerable contrast between the spectral performance of two "bad" bearings, J_2 and I, and two new, presumably "good" bearings. The mathematical model, described previously, was applied to the R4 bearing type and provided information regarding the location and identification of some of the peaks. For example, the major peaks expected for common defects in an R4 bearing, are summarized in Table 3.

A second method of spectral analysis was applied in an effort to develop a technique more easily adaptable to NARF requirements. This method involves analysis of the high frequency portion of the data. Impacts, resulting from damage or dirt in the test bearing can, under the proper conditions, excite the structural resonances of the test fixture. The excitation of such resonances is dependent upon the fundamental and harmonic frequencies of the impacts as well as the coupling between the bearing and the fixture. In our analysis, the fixture resonances at 32,000 Hz and 37,000 Hz were analyzed with respect to peak height and peak area.

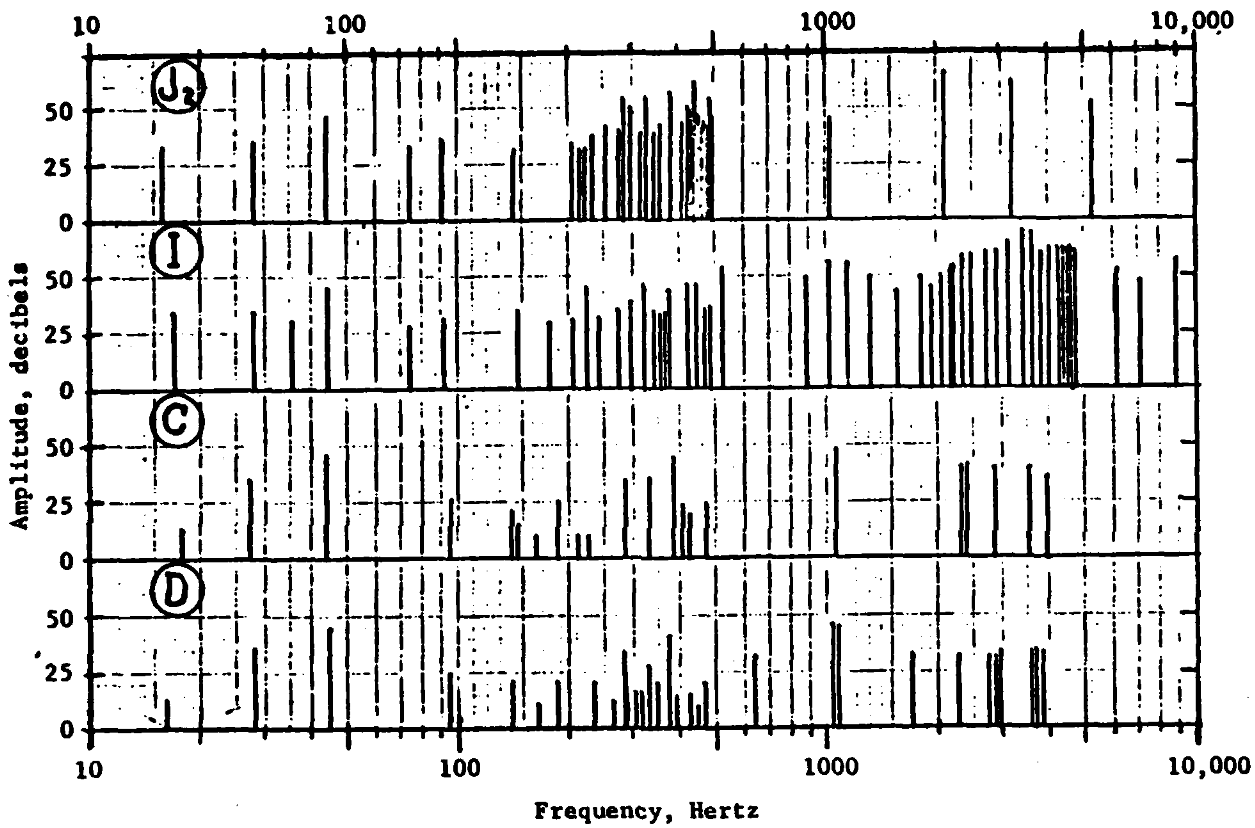

FIGURE 3. ACCELERATION SPECTRA FOR FOUR BEARINGS - 10 to 10,000 HZ

J_2 - Scratched outer race (New Departure)
I - "Failed" bearing (Barden)
C - New bearing (Barden)
D - New bearing (Barden)

Figure 4 illustrates the relative peak amplitudes for all bearings at 32,000 and at 37,000 Hz. The areas under the spectral plots over a frequency range, from 20,000 to 45,000 Hz are plotted in bar-graph form in Figure 5. All the results were normalized such that the average resonant-peak-area for the new bearings was unity. Corrections were made to the areas to account for the different amplification factors employed to record the raw data and to eliminate the artifact peaks* introduced by harmonic effects in the electronic components.

Results shown in Figure 4 are similarly normalized to the averaged linear amplitudes from the new bearings. Since the scale value for unity (new bearing average) is the same for both figures the graphed results are comparable in all respects.

DISCUSSION

Comparison of the high frequency region of the acceleration spectra appears to provide reasonably good discrimination between the "good" (new) and the "bad" (failed or damaged) bearings which were tested. Resonance peaks in the region above 5,000 Hz are due primarily to the structure of the fixture (32,000 Hz) or to the mounted resonance of the accelerometer (37,000 Hz). Thus it is reasonable to assume that peaks will occur in this region regardless of the particular vibration characteristics of a test bearing.

The relative performances based on resonance amplitude data (Figure 4), shows good discrimination for: "failed" Bearing I and for damaged Bearing J; fair discrimination for: "failed" Bearings E, F, G, and damaged Bearing B, and marginal discrimination for: "failed" Bearing H. Discriminations based on the data shown in Figure 5 appear to be more pronounced; however it should be recognized that frequency and amplitude normalizations were chosen so as to emphasize the relative differences.

---

*In the experimental data, spikes are presented in the amplitude/frequency plot at frequencies of 9500, 19,000, 29,000, 39,000, and 48,000 cps. These are introduced by the charge amplifier and were not due to the bearing.

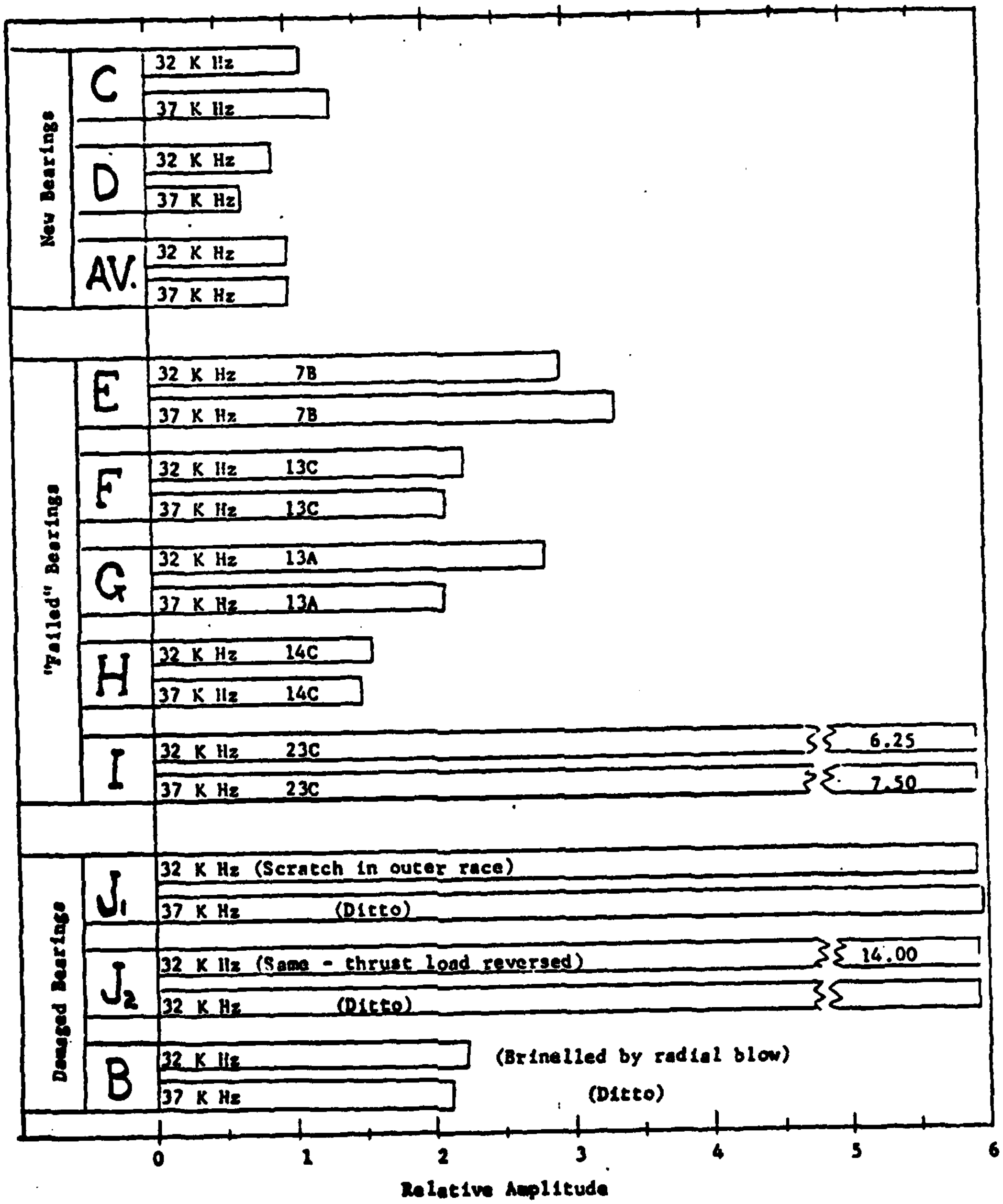

FIGURE 4. RELATIVE AMPLITUDES FOR 32,000 AND 37,000 HZ BEARING RESONANCES

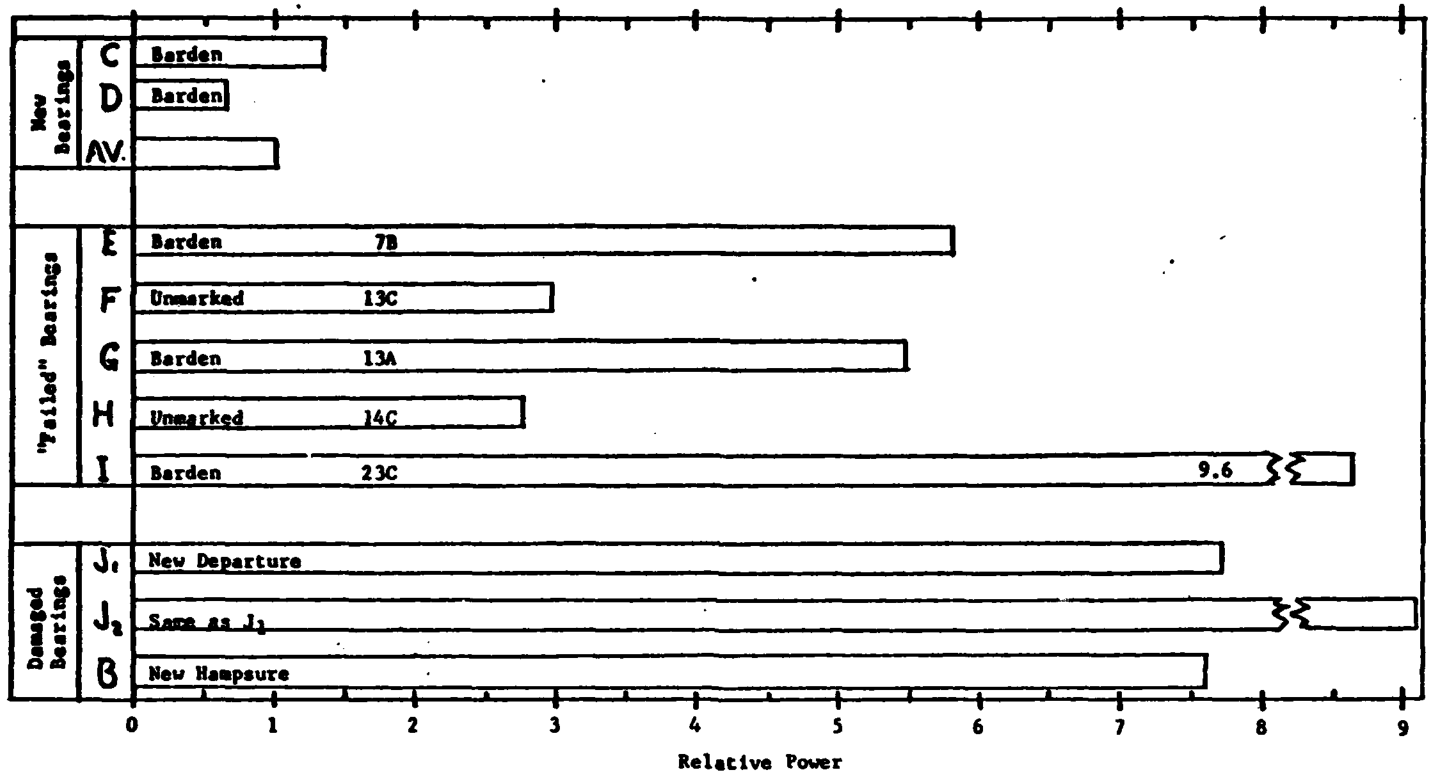

FIGURE 5. RELATIVE POWER FROM ACCELERATION SPECTRA FOR 20,000 TO 45,000 HZ RANGE

A study of fixture resonances was performed by sinusoidally exciting the fixture by an electrodynamic shaker. This indicated resonance peaks were present at approximately 1,000 Hz, 2,500 Hz, 3,000 Hz, 27,000 Hz, 32,000 Hz, and 37,000 Hz. In the approach used in the present series of experiments only the last two resonance peaks were evaluated and compared. There is a possibility, in some cases, that lower frequency peaks, e.g., 1000 Hz, 2500 Hz, or 3000 Hz, might be better indicators of bearing integritythan the high-range peaks which were chosen here. However, since the high frequency region is relatively free of extraneous noise, a better signal-to-noise ratio is obtained for the high frequency resonance peaks. Also lower frequency peaks may not be as broad in frequency as the high-range peaks and this might lower their effectiveness as discriminators.

CONCLUSIONS

It appears that the method of analysis of the high-frequency resonance peaks is most promising for application to acoustic characterization process for gyra and gyro bearings. Not only does this method appear to give the requisite discrimination between good and bad bearings, but it also can be adapted to relatively simple, inexpensive instrumentation. Once the real-time spectrum analyzer has been used to locate the critical resonance areas, the analyzer may be replaced by a simple band-pass filter and suitable integrating circuitry to give a simple go/no-go read out of bearing/gyro condition.

Full-scale implementation of the NDT method requires further development in two major areas:

- Development of a prototype test device for several commonly-used bearing types.
- The use of this device to screen and analyze a large population of bearings, both new and those which have failed other NARF nondestructive tests. The results of the acoustic method should be cross checked with other NDT results, such as torque tests, visual inspection, etc.

Then the results of this study must be analyzed with respect to the reliability of the method, and the suitability of the prototype unit for NARF service must be determined. A determination should be made as to how the new NDT method fits into the NARF program, and whether or not other tests can be waived when the acoustic method is implemented, etc.

In addition, an investigation to determine the suitability of the structural resonance method for the analysis of the condition of gyro buildups should be carried out. If the technique proves suitable, as we believe it will, then a powerful tool for monitoring the condition of bearings throughout the assembly of the gyro can be developed.

ACKNOWLEDGEMENTS

The authors gratefully acknowledge the contributions of Dr. Donald Houser of The Ohio State University, Department of Engineering.

REFERENCES

(1) L. F. Sturgeon, D. K. Snediker, and S. M. Weinberger, "Characterization of Miniature Ball Bearings by Acoustic Signature Analysis", Proceedings of the 17th Meeting of the Mechanical Failures Prevention Group, November 1, 1972.

(2) L. F. Sturgeon, "Acoustic Characterization of Precision Ball Bearings", International Ball Bearing Symposium, Cambridge, Mass., June, 1973.

(3) J. J. Broderick, R. F. Burchill, and H. L. Clark, "Design and Fabrication of a Prototype System for Early Warning of Impending Bearing Failures", George C. Marshall Space Flight Center, MFS-21877, January, 1972.

(4) J. J. Anderson and A. S. Babkin, "Mechanical Signature Analysis of Ball Bearings by Real Time Spectrum Analysis", 18th Annual Meeting, Institute of Environmental Sciences, N. Y., May, 1972.

(5) H. C. Rippel and J. H. Rumbarger, "An Analytical and Experimental Study of the Structureborn and Airborn Vibration of Rolling Element and Sliding Surface Bearings", Department of the Navy, Bureau of Ships, Contract No. NObs-77184, March, 1966.

(6) B. Weichbrodt and F. J. Bowden, "Instrumentation for Predicting Bearing Damage", Rome Air Development Center, Air Force Systems Command, Griffiss Air Force Base, N.Y., March, 1970.

(7) H. L. Balderston, "Detection of Incipient Failure in Bearings", <u>Materials Evaluation</u>, June, 1969, p. 123.

END

DATE
FILMED
11-81

DTIC